Supporting Information for

An immunogenic anti-cancer stem cell bi-nuclear copper(II)-flufenamic acid complex

Yue Li,[a,†] Jiaxin Fang,[a,†] Kuldip Singh,[a] Fabrizio Ortu*[a] and Kogularamanan Suntharalingam*[a]

[a] School of Chemistry, University of Leicester, Leicester, LE1 7RH, United Kingdom;
† These authors contributed equally to this work

* To whom correspondence should be addressed:
Email: k.suntharalingam@leicester.ac.uk; fabrizio.ortu@leicester.ac.uk

Table of Content

Experimental

Experimental Section.

Materials and methods. All synthetic procedures were performed under normal atmospheric conditions. Fourier transform infrared (FTIR) spectra were recorded with an IRAffinity-1S Shimadzu spectrophotometer. UV-vis absorption spectra were recorded on a Cary 3500 UV-vis spectrophotometer. Elemental analysis of the compounds prepared was performed commercially by the University of Cambridge. $CuCl_2•2H_2O$, 1,10-phenanthroline, 3,4,7,8-tetramethyl-1,10-phenanthroline, and flufenamic acid were purchased from Sigma Aldrich and used as received.

Synthesis of [Cu(1,10-phenanthroline)(flufenamate)$_2$](1). KOH (25 mg, 0.45 mmol) was added to a solution of flufenamic acid (100 mg, 0.36 mmol) in methanol (4 mL). This solution was stirred at room temperature for 1 h. Methanolic solutions (2 mL each) of 1,10-phenanthroline (32 mg, 0.18 mmol) and $CuCl_2•2H_2O$ (31 mg, 0.18 mmol) were then simultaneously added to the solution containing flufenamic acid, and the dark green mixture was stirred at 50 °C for 20 h. The resulting precipitate was filtered off, and the filtrate was evaporated to dryness. The resultant solid was washed thoroughly with water (3 x 20 mL) and diethyl ether (3 x 20 mL) to yield pure **1** as a green solid (86 mg, 59%); IR (solid, cm^{-1}): 3254, 1607, 1580, 1520, 1492, 1426, 1380, 1331, 1284, 1237, 1185, 1157, 1110, 1063, 997, 931, 869, 850, 780, 766, 723, 695, 671, 624, 563, 523, 455, 430, 412; HR ESI-MS Calcd. for $C_{40}H_{26}CuF_6N_4O_4Na$ [**1**+Na]$^+$: 826.1052 a.m.u. Found 826.1053 a.m.u.; Anal. Calcd. for **1**, $C_{40}H_{26}CuF_6N_4O_4•H_2O$: C, 58.43; H, 3.43; N: 6.81. Found: C, 58.75; H, 3.11; N, 6.81.

Synthesis of [Cu(3,4,7,8-tetramethyl-1,10-phenanthroline)(methanol)(μ-flufenamate)(μ-OH)Cu(3,4,7,8-tetramethyl-1,10-phenanthroline)(flufenamate)][flufenamate] (2). KOH (25 mg, 0.45 mmol) was added to a solution of flufenamic acid (100 mg, 0.36 mmol) in methanol (4 mL). This solution was stirred at room temperature for 1 h. Methanolic solutions (2 mL each) of 3,4,7,8-tetramethyl-1,10-phenanthroline (43 mg, 0.18 mmol) and $CuCl_2•2H_2O$ (31 mg, 0.18 mmol) were then simultaneously added to the solution containing flufenamic acid, and the dark green mixture was stirred at 50 °C for 20 h. The resulting precipitate was filtered off, and the filtrate was evaporated to dryness. The resultant solid was washed thoroughly with water (3 x 20 mL) and diethyl ether (3 x 20 mL) to yield pure **2** as a green solid (77 mg, 57%); IR (solid, cm^{-1}): 3255, 3066, 1588, 1510, 1461, 1430, 1378, 1330, 1284, 1159, 1116, 1069, 997, 929, 793, 749, 722, 695, 661, 552, 455, 412; HR ESI-MS Calcd. for $C_{74}H_{59}Cu_2F_9N_7O_6$ [**2**-MeOH-OH]$^+$: 1440.2980 a.m.u. Found 1440.3016 a.m.u.; Anal. Calcd. for **2**, $C_{75}H_{64}Cu_2F_9N_7O_8$: C, 60.48; H, 4.33; N: 6.58. Found: C, 60.11; H, 3.92; N, 6.34.

X-ray crystallography. The crystal data for all compounds are compiled in Tables S1–S3. Crystals were mounted in inert oil on micromounts and examined using a Bruker D8 Quest diffractometer with a Photon III detector and a microfocus source with Cu-Kα radiation (λ = 1.54178) at 150(2) K. Intensities were integrated from data recorded on 1° frames by ω or φ rotation. A multi-scan method absorption correction with a beam profile was applied.[1] The structures were solved using SHELXS[2] or SHELXT;[3] the datasets were refined by full-matrix least-squares on reflections with $F^2 \geq 2\sigma(F^2)$ values, with anisotropic displacement parameters for all non-hydrogen atoms, and with constrained riding hydrogen geometries;[2] U_{iso}(H) was set at 1.2 (1.5 for methyl groups) times U_{eq} of the parent atom. The largest features in final difference syntheses were close to heavy atoms and were of no chemical significance. SHELX[2,3] was employed through OLEX2 for structure solution and refinement.[4] ORTEP-3[5] and POV-Ray[6] were employed for molecular graphics. The CCDC deposition numbers

2324436-2324437 contain the supplementary crystallographic data. This data can be obtained free of charge via The Cambridge Crystallography Data Centre.

Measurement of water-octanol partition coefficient (LogP). The LogP value for **1** and **2** was determined using the shake-flask method and UV-vis spectroscopy. The 1-octanol used in this experiment was pre-saturated with water. A DMSO solution of **1** or **2** (10 μL, 10 mM) was incubated with 1-octanol (495 μL) and H_2O (495 μL) in a 1.5 mL tube. The tube was shaken at room temperature for 24 h. The two phases were separated by centrifugation and the content of **1** or **2** in the water and 1-octanol phases was determined by UV-vis spectroscopy.

Cell culture. The human mammary epithelial cell lines, HMLER and HMLER-shEcad were kindly donated by Prof. R. A. Weinberg (Whitehead Institute, MIT). HMLER and HMLER-shEcad cells were maintained in Mammary Epithelial Cell Growth Medium (MEGM) with supplements and growth factors (BPE, hydrocortisone, hEGF, insulin, and gentamicin/amphotericin-B). The BEAS-2B bronchial epithelium cell line was acquired from American Type Culture Collection (ATCC, Manassas, VA, USA) and cultured in RPMI 1640 medium with 2 mM L-glutamine supplemented with 1% penicillin and 10% fetal bovine serum. The cells were grown at 310 K in a humidified atmosphere containing 5% CO_2.

Cytotoxicity studies: MTT assay. Exponentially growing cells were seeded at a density of approximately 5×10^3 cells per well in 96-well flat-bottomed microplates and allowed to attach for 24 h prior to addition of compounds. Various concentrations of the test compounds (0.0004-100 μM) were added and incubated for 72 h at 37 °C (total volume 200 μL). Stock solutions of the compounds were prepared as 10 mM DMSO solutions and diluted using cell media. The final concentration of DMSO in each well was ≤1 %. After 72 h, 20 μL of MTT (4 mg mL^{-1} in PBS) was added to each well and the plates incubated for an additional 4 h at 37 °C. The media/MTT mixture was eliminated and DMSO (100 μL per well) was added to dissolve the formazan precipitates. The optical density was measured at 550 nm using a 96-well multiscanner autoreader. Absorbance values were normalised to (DMSO-containing) control wells and plotted as concentration of compound versus % cell viability. IC_{50} values were interpolated from the resulting dose dependent curves. The reported IC_{50} values are the average of three independent experiments (n = 18).

Tumorsphere formation and viability assay. HMLER-shEcad cells (5×10^3) were plated in ultralow-attachment 96-well plates (Corning) and incubated in MEGM supplemented with B27 (Invitrogen), 20 ng mL^{-1} EGF and 4 μg mL^{-1} heparin (Sigma) for 5 days. Studies were also conducted in the presence of **1**, **2**, flufenamic acid, cisplatin, and salinomycin (0-133 μM). Mammospheres treated with **1**, **2**, flufenamic acid, cisplatin, and salinomycin (at their respective IC_{20} values, 5 days) were counted and imaged using an inverted microscope. The viability of the mammospheres was determined by addition of a resazurin-based reagent, TOX8 (Sigma). After incubation for 16 h, the fluorescence of the solutions was read at 590 nm (λ_{ex} = 560 nm). Viable mammospheres reduce the amount of the oxidised TOX8 form (blue) and concurrently increase the amount of the fluorescent TOX8 intermediate (red), indicating the degree of mammosphere cytotoxicity caused by the test compound. Fluorescence values were normalised to DMSO-containing controls and plotted as concentration of test compound versus % mammosphere viability. IC_{50} values were interpolated from the resulting dose dependent curves. The reported IC_{50} values are the average of two independent experiments, each consisting of two replicates per concentration level (n = 4).

Cellular uptake. To measure the cellular uptake of **2**, about 1 million HMLER-shEcad cells were treated with **2** (1 μM) at 37 °C for 24 h. After incubation, the media was removed, the

cells were washed with PBS (2 mL × 3) and harvested. The number of cells was counted at this stage, using a haemocytometer. This mitigates any cell death induced by **2** at the administered concentration and experimental cell loss. Half of the cellular pellet was dissolved in 65% HNO_3 (250 µL) overnight. Half of the cellular pellet was used to determine the copper content in the cytoplasmic, nuclear, and membrane fractions. The Thermo Scientific NE-PER Nuclear and Cytoplasmic Extraction Kit was used to extract and separate the cytoplasmic, nuclear, and membrane fractions. The fractions were dissolved in 65% HNO_3 (250 µL final volume) overnight. All samples were diluted 17-fold with water and analysed using inductively coupled plasma mass spectrometry (ICP-MS, Thermo Scientific ICAP-Qc quadrupole ICP mass spectrometer). Copper levels are expressed as mass of Cu (ng) per million cells. Results are presented as the mean of three determinations for each data point.

Intracellular ROS assay. HMLER-shEcad cells (5×10^3) were seeded in each well of a 96-well plate. After incubating the cells overnight, they were treated with **2** ($2 \times IC_{50}$ value for 0.5-24 h), and incubated with 6-carboxy-2′,7′-dichlorodihydrofluorescein diacetate (20 µM) for 30 min. The intracellular ROS level was determined by measuring the fluorescence of the solutions in each well at 529 nm (λ_{ex} = 504 nm).

Immunoblotting analysis. HMLER-shEcad cells (1×10^6) were incubated with **2** (0.5-2 µM for 48 h) at 37 °C. HMLER-shEcad cells were harvested and isolated as pellets. SDS-PAGE loading buffer (64 mM Tris-HCl (pH 6.8), 9.6% glycerol, 2% SDS, 5% β-mercaptoethanol, 0.01% bromophenol blue) was added to the pellets, and this was incubated at 95 °C for 10 min. Cell lysates were resolved by 4-20 % sodium dodecylsulphate polyacylamide gel electrophoresis (SDS-PAGE; 200 V for 25 min) followed by electro transfer to polyvinylidene difluoride membrane, PVDF (350 mA for 1 h). Membranes were blocked in 5% (w/v) non-fat milk in PBST (PBS/0.1% Tween 20) and incubated with the appropriate primary antibodies (Cell Signalling Technology). After incubation with horseradish peroxidase-conjugated secondary antibodies (Cell Signalling Technology), immune complexes were detected with the ECL detection reagent (BioRad) and analysed using a chemiluminescence imager (Bio-Rad ChemiDoc Imaging System).

Annexin V-propidium iodide assay. HMLER-shEcad cells were incubated with and without **2** ($2 \times IC_{50}$ value or $4 \times IC_{50}$ value for 72 h) and cisplatin (25 µM for 72 h) at 37 °C. Cells were harvested from adherent cultures by trypsinisation. The FITC Annexin V/Dead Cell Apoptosis Kit was used. The manufacture's (Thermo Fisher Scientific) protocol was followed to carry out this experiment. Briefly, untreated and treated cells (1×10^6) were suspended in 1× Annexin binding buffer (100 µL) (10 mM HEPES, 140 mM NaCl, 2.5 mM $CaCl_2$, pH 7.4), then 5 µL of FITC Annexin V and 1 µL of PI (100 µg/ mL) were added to each sample and incubated at room temperature for 15 min. After which more 1× Annexin binding buffer (400 µL) was added while gently mixing. The cells were analysed using a FACSCanto II flow cytometer (BD Biosciences) (10,000 events per sample were acquired) at the University of Leicester FACS Facility. The FL1 channel was used to assess Annexin V binding and the FL2 channel was used to assess PI uptake. Cell populations were analysed using the FlowJo software (Tree Star).

COX-2 expression assay. HMLER-shEcad cells were seeded in 6-well plates (at a density of 5×10^5 cells/ mL) and the cells were allowed to attach overnight. The cells were treated with lipopolysaccharide (LPS) (2.5 µM for 24 h), and then treated with **2** ($2 \times IC_{50}$ value) or flufenamic acid (20 µM) and incubated for a further 48 h. The cells were then harvested by trypsinisation, fixed with 4% paraformaldehyde (at 37 °C for 10 min), permeabilised with ice-cold methanol (for 30 min), and suspended in PBS (200 µL). The Alexa Fluor® 488 nm

labelled anti-COX-2 antibody (2 μL) was then added to the cell suspension and incubated in the dark for 1 h. The cells were then washed with PBS (1 mL) and analysed using a FACSCanto II flow cytometer (BD Biosciences) (10,000 events per sample were acquired) at the University of Leicester FACS Facility. The FL1 channel was used to assess COX-2 expression. Cell populations were analysed using the FlowJo software (Tree Star).

CRT cell surface exposure. Flow cytometry was used to analyse cell surface CRT exposure. HMLER-shEcad cells were seeded into a 6-well plate (at a density of 5×10^5 cells/ mL) and the cells were incubated at 37 °C overnight. The cells were treated with **2** (3 μM or 6 μM) or co-treated with cisplatin (150 μM) with thapsigargin (7 μM) for 24 h at 37 °C. The cells were then harvested by trypsinization and collected by centrifugation. The resulting pellets were suspended in PBS (500 μL), and after the addition of the Alexa Fluor® 488 nm labelled anti-CRT antibody (2 μL), the cells were incubated in the dark for 30 minutes. The cells were then washed with PBS (1 mL) and analysed using a FACSCanto II flow cytometer (BD Biosciences) (10,000 events per sample were acquired) at the University of Leicester FACS Facility. The FL1 channel was used to assess CRT cell surface exposure.

ATP assay. HMLER-shEcad cells (5×10^3 cells /well) were seeded in a 96-well plate and incubated overnight. The cells were then treated with **2** (IC_{50} value, $2 \times IC_{50}$ value or $4 \times IC_{50}$ value) or cisplatin (50 μM, positive control) for 24 h at 37 °C. The media was carefully extracted and transferred into a white-walled opaque 96-well plate, and a luciferin-based ENLITEN ATP Assay Kit (Promega) was used to measure the relative amount of ATP released into the supernatant.

HMGB-1 release. HMLER-shEcad cells (1×10^6 cells) were incubated with **2** (0.5-2 μM) for 48 h at 37 °C. Cells were collected in full and added to SDS-PAGE loading buffer (64 mM Tris-HCl (pH 6.8), 9.6% glycerol, 2% SDS, 5% β-mercaptoethanol, 0.01% Bromophenol Blue) and incubated at 95 °C for 10 min. The HMGB-1 content was probed by immunoblotting analysis as described above. The anti-HMGB-1 antibody (Cell Signalling Technology) was used in this experiment.

Phagocytosis assay. HMLER-shEcad cells were seeded into a 6-well plate (at a density of 5×10^5 cells/ mL) and the cells were incubated at 37 °C overnight. The cells were stained with CellTracker Green (30 min) and washed with MEGM media. The cells were then treated with **2** (5 μM), flufenamic acid (20 μM) or cisplatin (150 μM) with thapsigargin (7 μM) for 24 h at 37 °C. Then macrophages, obtained by differentiating THP-1 cells with phorbol 12-myristate 13-acetate (100 nM for 72 h) and pre-stained with CellTracker Orange for 30 min and washed with RPMI 1640 media, were added to the HMLER-shEcad cells (at a density of 5×10^5 cells/ mL). After 2 h, phagocytosis was assessed by flow cytometry, using a FACSCanto II flow cytometer (BD Biosciences) (10,000 events per sample were acquired) at the University of Leicester FACS Facility. The FL1 channel was used to assess the CellTracker Green-stained HMLER-shEcad cell population and the FL4 channel was used to assess the CellTracker Orange-stained THP-1 macrophage population. Cell populations were analysed using the FlowJo software (Tree Star).

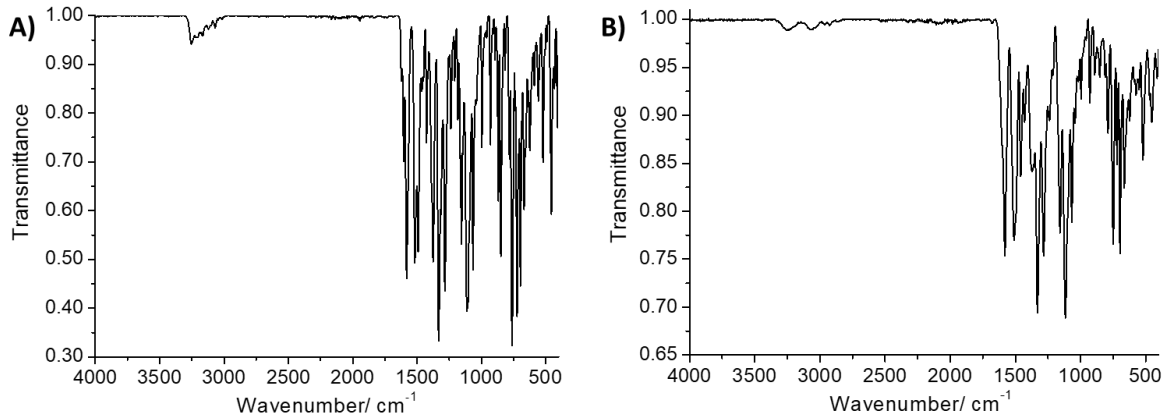

Fig. S1 ATR-FTIR spectra of (A) **1** and (B) **2** in the solid form.

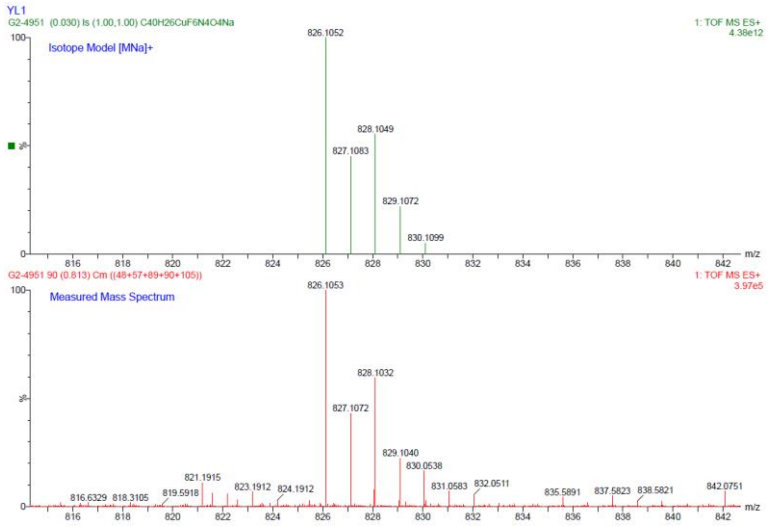

Fig. S2 (Top) Theoretical isotope model for [**1**+Na]$^+$ ($C_{40}H_{26}CuF_6N_4O_4Na$) and (bottom) the experimentally determined high-resolution ESI-TOF mass spectrum for complex **1**.

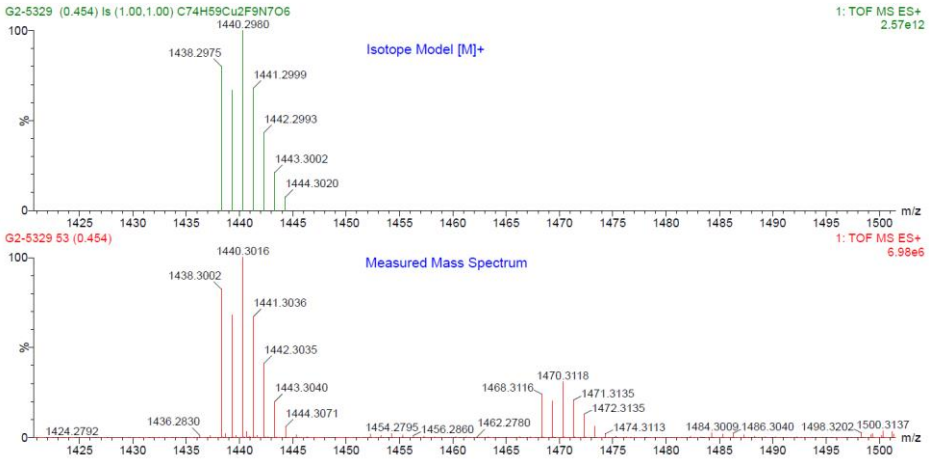

Fig. S3 (Top) Theoretical isotope model for [**2**-MeOH-OH]$^+$ ($C_{74}H_{59}Cu_2F_9N_7O_6$) and (bottom) the experimentally determined high-resolution ESI-TOF mass spectrum for complex **2**.

Table S1. Selected crystallographic data for complexes **1** and **2**.

Metal complex	**1**	**2**
CCDC No.	2324436	2324437
formula	$C_{40}H_{26}CuF_6N_4O_4$	$C_{75}H_{64}Cu_2F_9N_7O_8$
w	804.19	1489.41
Crystal system	monoclinic	triclinic
Space group	*C2/c*	*P-1*
a, Å	12.2780(4)	12.4413(3)
b, Å	10.4444(3)	17.2045(4)
c, Å	26.2613(8)	17.6456(4)
α, deg.	90	107.9390(10)
β, deg.	93.9570(10)	97.4370(10)
γ, deg.	90	101.8340(10)
V, Å^3	3359.62(18)	3440.93(14)
Z	4	2
ρ_{calc}g/cm^3	1.590	1.438
2*θ* / deg.	6.748 to 144.314	5.38 to 144.744
Reflections collected	19056	69369
Independent reflections	3275	13504
Goodness-of-fit on F^2	1.082	1.033
R_1, wR_2 [$I \geq 2\sigma(I)$]	0.0304, 0.0755	0.0549, 0.1459
R_1, wR_2 [all data]	0.0305, 0.0756	0.0709, 0.1594
Largest diff. peak/hole / e Å^{-3}	0.35, -0.37	0.98, -0.56

Table S2. Selected bond lengths (Å) and angles (°) for complex **1**.

Cu(1)-O(1)	1.9455(11)	Cu(1)-N(2)	2.0026(13)
Cu(1)-O(1)^{i}	1.9455(11)	Cu(1)-N(2)^{i}	2.0026(13)
O(1)-Cu(1)-O(1)^{i}	93.82(7)	O(1)^{i}-Cu(1)-N(2)^{i}	172.09(5)
O(1)-Cu(1)-N(2)^{i}	92.34(5)	O(1)^{i}-Cu(1)-N(2)	92.34(5)
O(1)-Cu(1)-N(2)	172.09(5)	N(2)-Cu(1)-N(2)^{i}	81.99(8)

Table S3. Selected bond lengths (Å) and angles (°) for complex **2**.

Cu(1)-O(1)	1.8963(19)	Cu(2)-O(1)	1.9017(19)
Cu(1)-O(2)	1.924(2)	Cu(2)-O(5)	1.976(2)
Cu(1)-O(4)	2.389(2)	Cu(2)-O(6)	2.287(2)
Cu(1)-N(1)	2.002(2)	Cu(2)-N(4)	2.026(3)
Cu(1)-N(2)	2.027(2)	Cu(2)-N(5)	2.011(2)
O(1)-Cu(1)-O(2)	95.64(9)	O(1)-Cu(2)-O(5)	91.07(9)
O(1)-Cu(1)-O(4)	84.89(8)	O(1)-Cu(2)-O(6)	94.56(9)
O(1)-Cu(1)-N(1)	92.95(10)	O(1)-Cu(2)-N(4)	95.60(10)
O(1)-Cu(1)-N(2)	173.98(10)	O(1)-Cu(2)-N(5)	167.54(10)
O(2)-Cu(1)-O(4)	90.63(9)	O(5)-Cu(2)-O(6)	92.74(9)
O(2)-Cu(1)-N(1)	171.37(9)	O(5)-Cu(2)-N(4)	168.73(10)
O(2)-Cu(1)-N(2)	90.36(10)	O(5)-Cu(2)-N(5)	90.58(10)
N(1)-Cu(1)-O(4)	90.91(8)	N(4)-Cu(2)-O(6)	95.76(10)
N(1)-Cu(1)-N(2)	81.05(10)	N(5)-Cu(2)-O(6)	97.69(9)
N(2)-Cu(1)-O(4)	95.56(8)	N(5)-Cu(2)-N(4)	80.97(10)

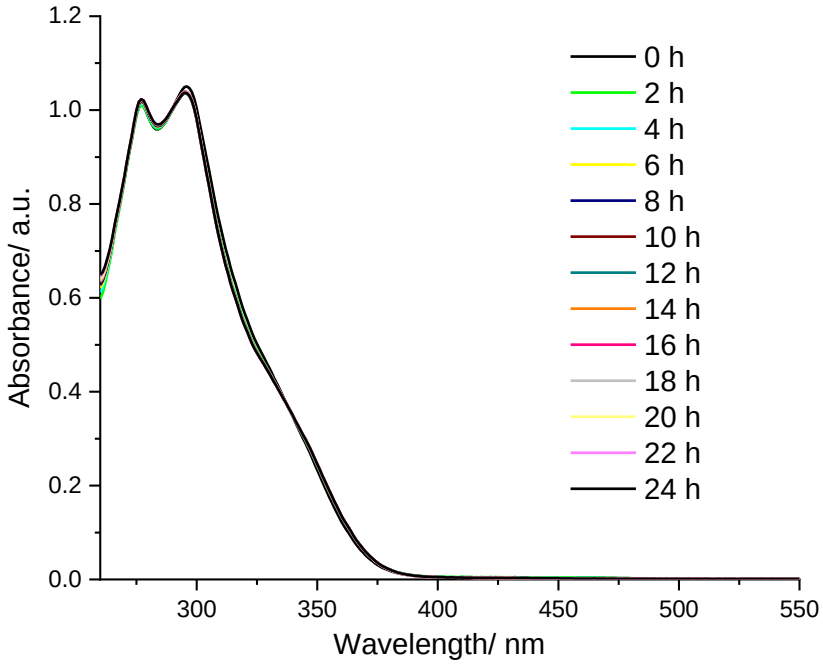

Fig. S4 UV-vis spectra of **1** (25 μM) in DMSO over the course of 24 h at 37 °C.

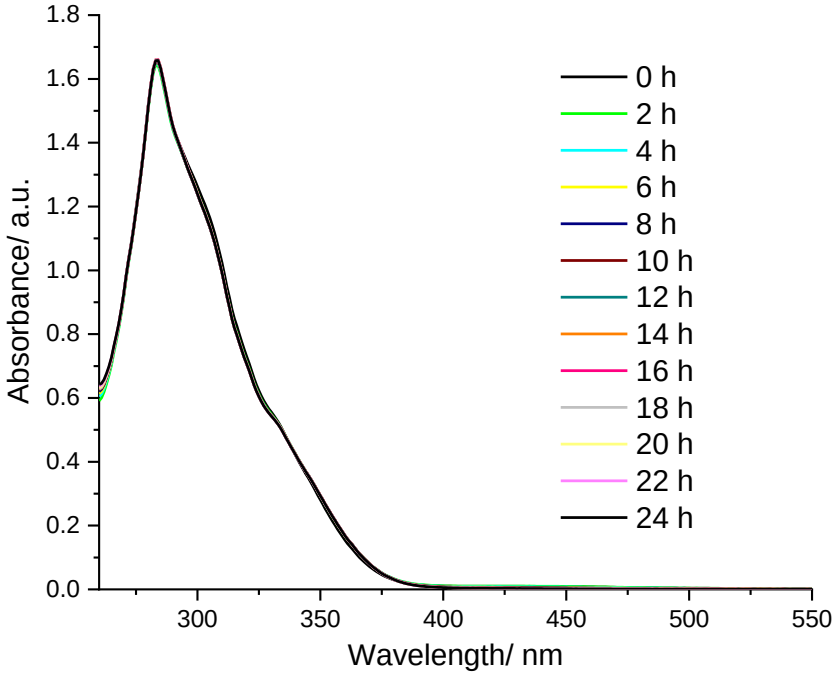

Fig. S5 UV-vis spectra of **2** (25 μM) in DMSO over the course of 24 h at 37 °C.

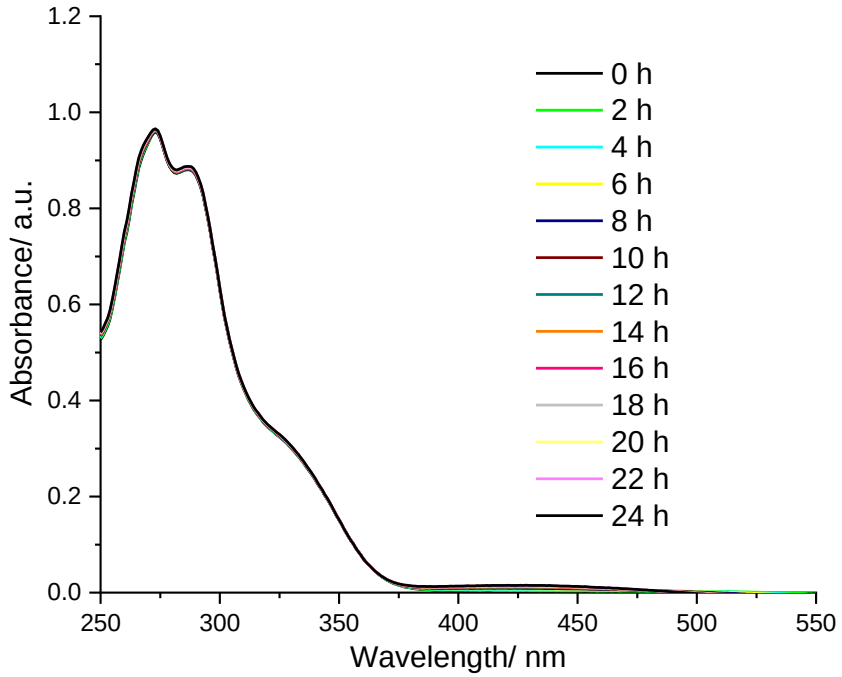

Fig. S6 UV-vis spectra of **1** (25 μM) in mammary epithelial cell growth medium (MEGM):DMSO (95:5) over the course of 24 h at 37 °C.

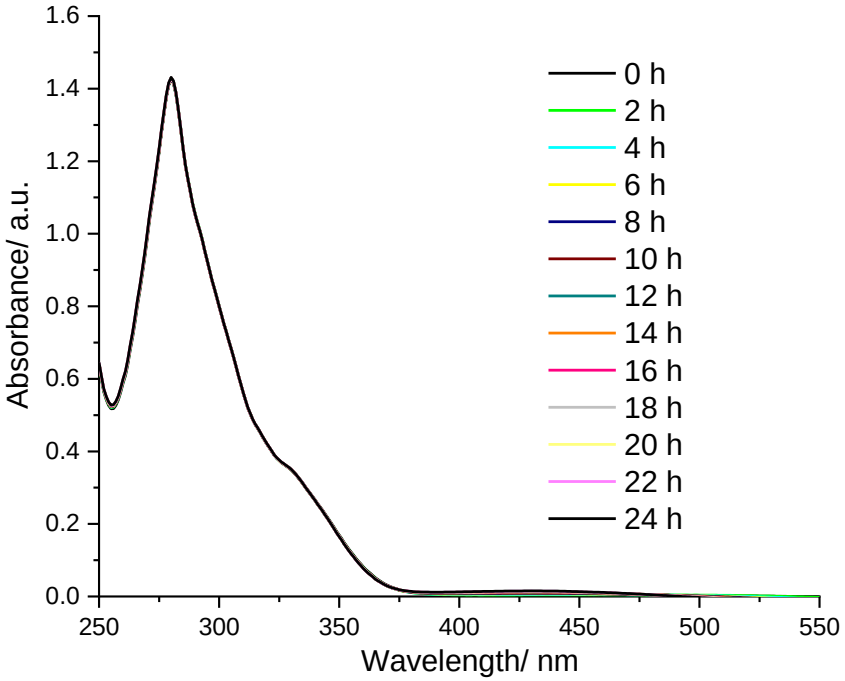

Fig. S7 UV-vis spectra of **2** (25 μM) in mammary epithelial cell growth medium (MEGM):DMSO (95:5) over the course of 24 h at 37 °C.

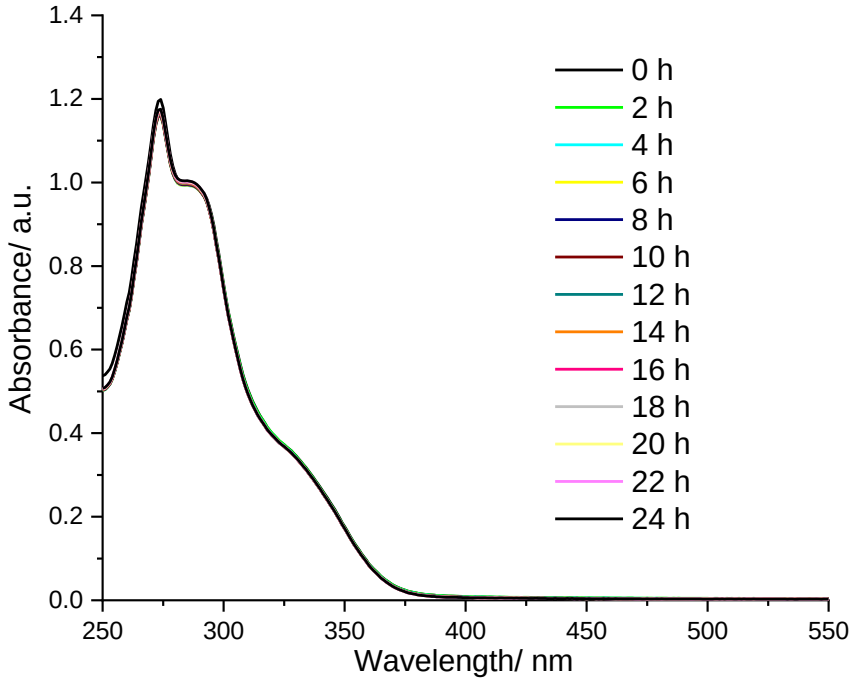

Fig. S8 UV-vis spectra of **1** (25 μM) in the presence of ascorbic acid (250 μM) in PBS:DMSO (95:5) over the course of 24 h at 37 °C.

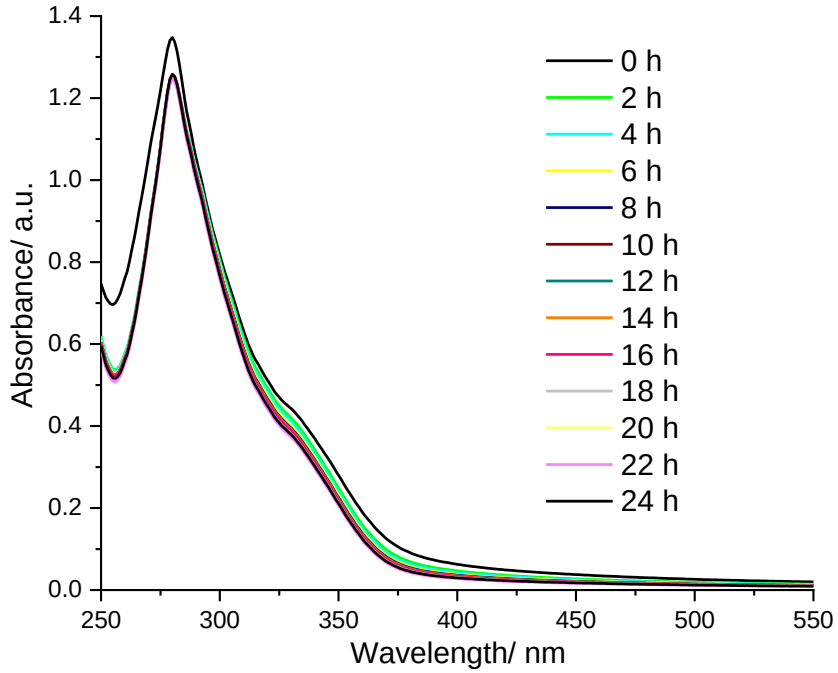

Fig. S9 UV-vis spectra of **2** (25 μM) in the presence of ascorbic acid (250 μM) in PBS:DMSO (95:5) over the course of 24 h at 37 °C.

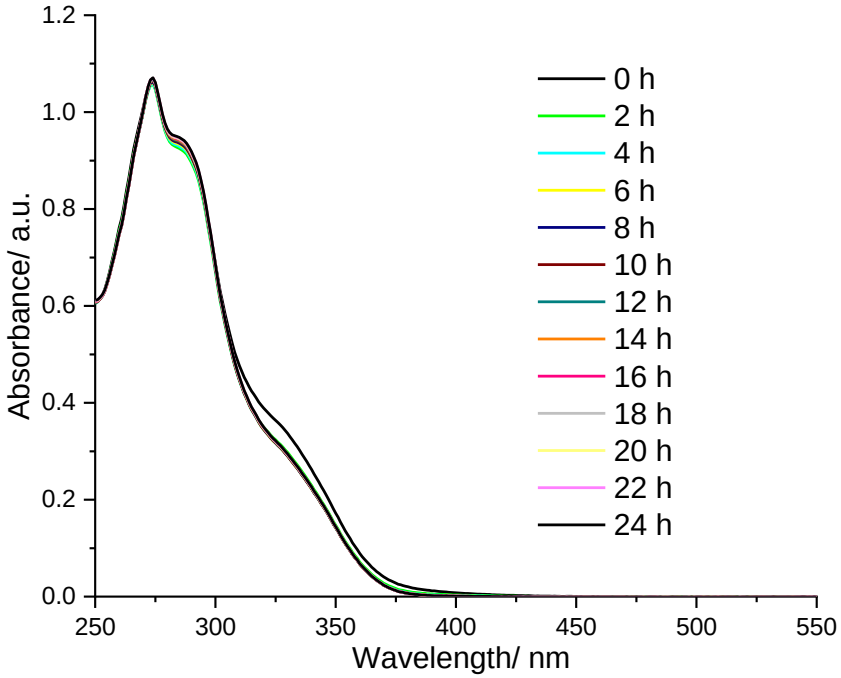

Fig. S10 UV-vis spectra of **1** (25 μM) in the presence of glutathione (250 μM) in PBS:DMSO (95:5) over the course of 24 h at 37 °C.

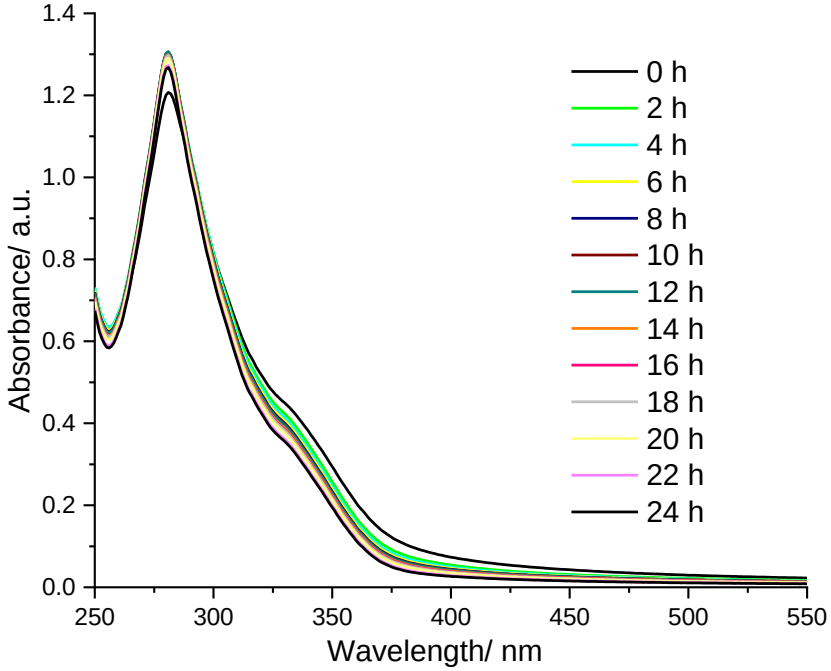

Fig. S11 UV-vis spectra of **2** (25 μM) in the presence of glutathione (250 μM) in PBS:DMSO (95:5) over the course of 24 h at 37 °C.

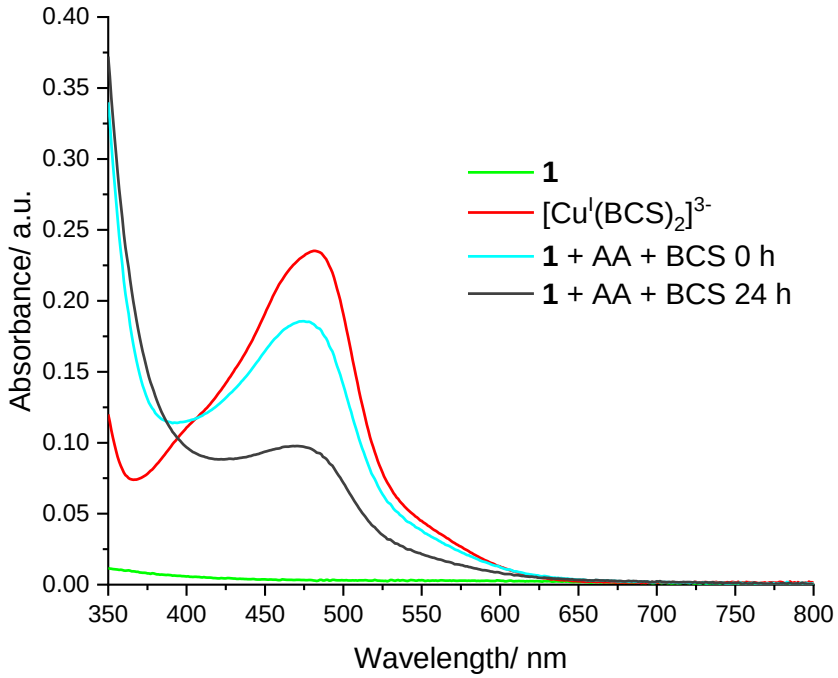

Fig. S12 UV-vis spectra of **1** (25 μM) in the presence of ascorbic acid (250 μM) and bathocuproine disulfonate, BCS (50 μM) in PBS:DMSO (95:5) over the course of 24 h at 37 ^{o}C.

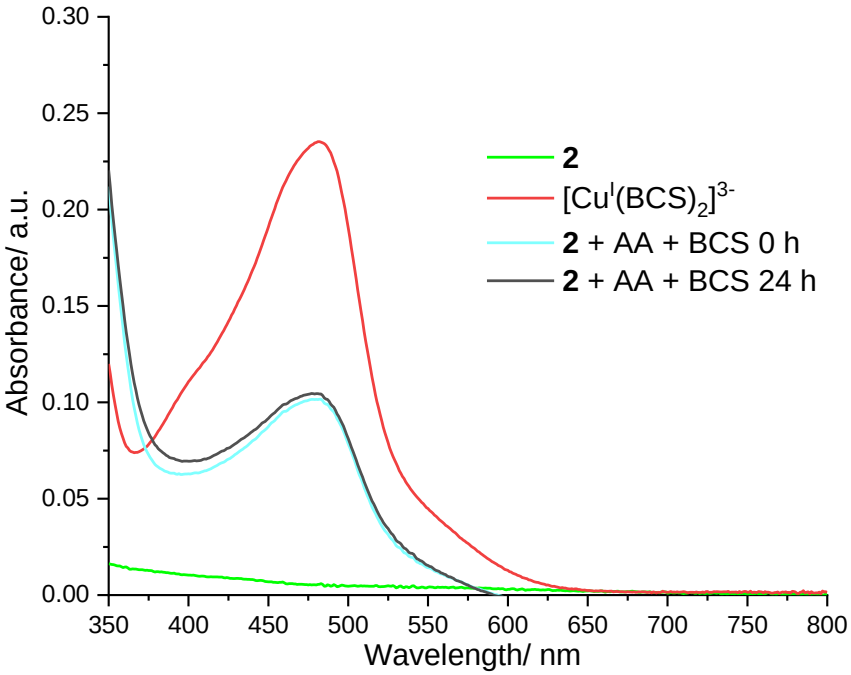

Fig. S13 UV-vis spectra of **2** (25 μM) in the presence of ascorbic acid (250 μM) and bathocuproine disulfonate, BCS (50 μM) in PBS:DMSO (95:5) over the course of 24 h at 37 ^{o}C.

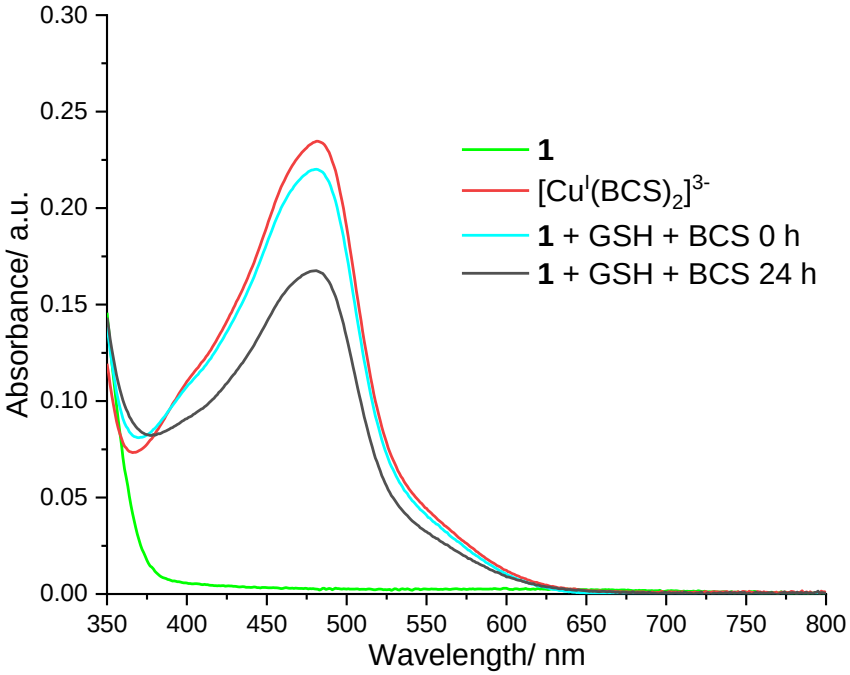

Fig. S14 UV-vis spectra of **1** (25 μM) in the presence of glutathione (250 μM) and bathocuproine disulfonate, BCS (50 μM) in PBS:DMSO (95:5) over the course of 24 h at 37 ^{o}C.

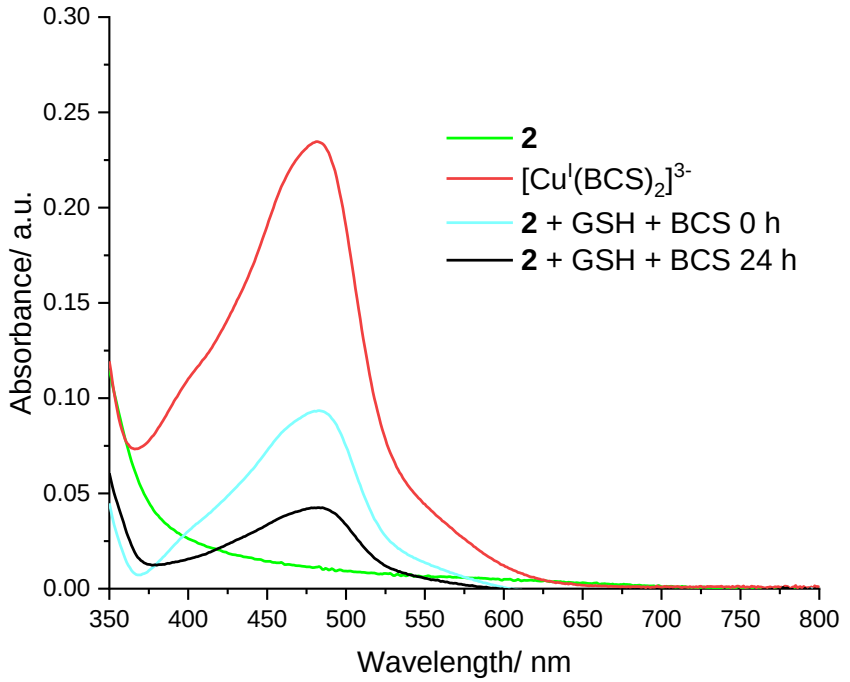

Fig. S15 UV-vis spectra of **2** (25 μM) in the presence of glutathione (250 μM) and bathocuproine disulfonate, BCS (50 μM) in PBS:DMSO (95:5) over the course of 24 h at 37 ^{o}C.

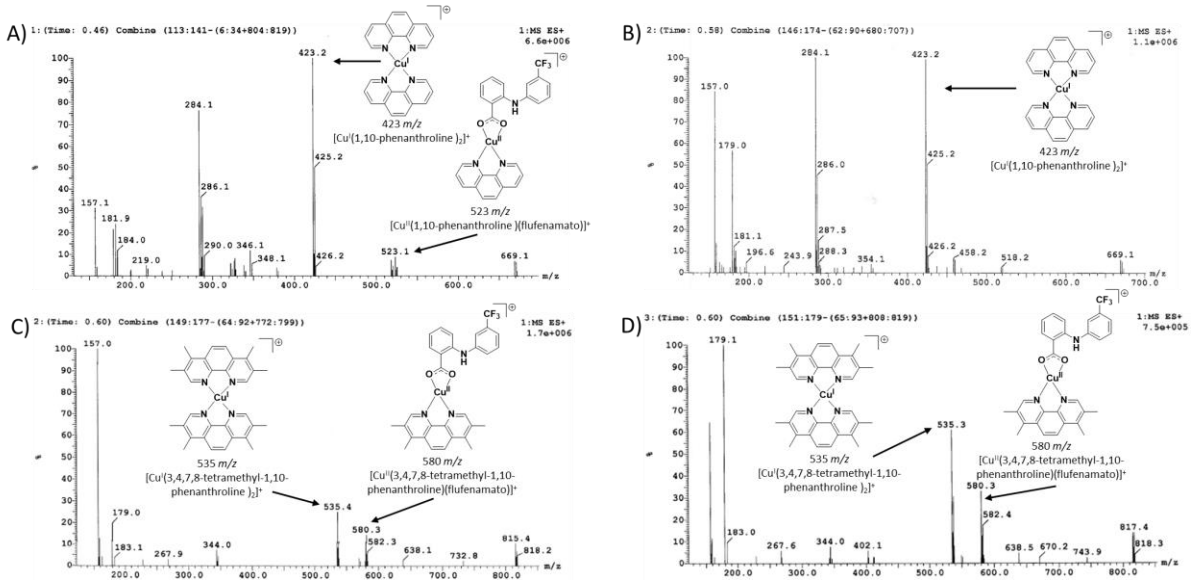

Fig. S16 ESI mass spectrum (positive mode) of **1** (500 μM) in H_2O:DMSO (10:1) at 37 ^oC in the presence of ascorbic acid (5 mM) after (A) 0 h and (B) 24 h incubation. ESI mass spectrum (positive mode) of **2** (500 μM) in H_2O:DMSO (10:1) at 37 ^oC in the presence of ascorbic acid (5 mM) after (C) 0 h and (D) 24 h incubation.

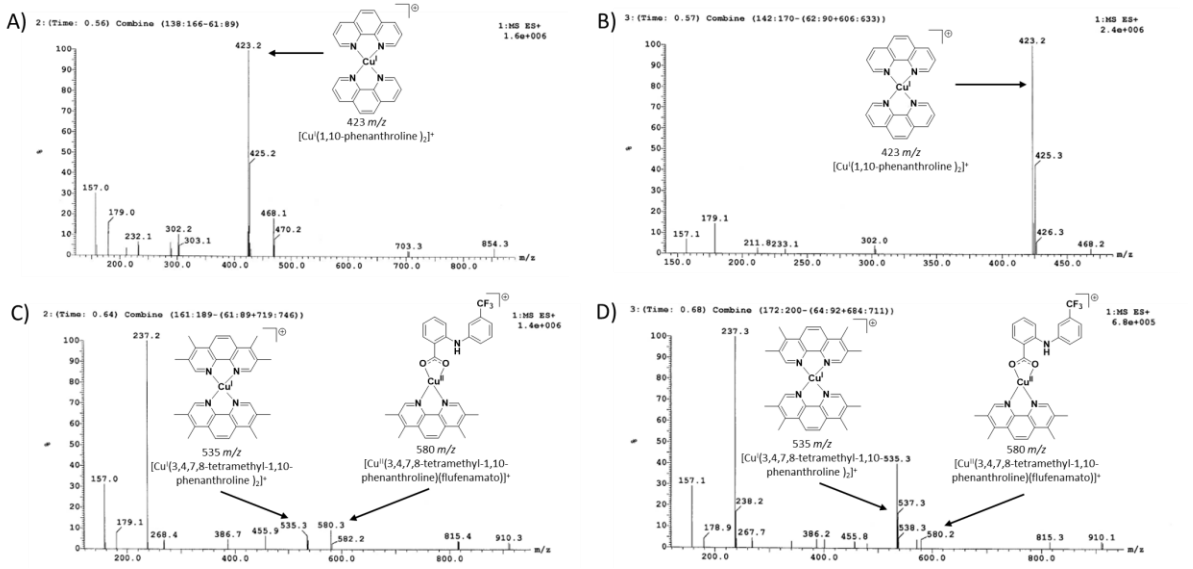

Fig. S17 ESI mass spectrum (positive mode) of **1** (500 μM) in H_2O:DMSO (10:1) at 37 ^oC in the presence of glutathione (5 mM) after (A) 0 h and (B) 24 h incubation. ESI mass spectrum (positive mode) of **2** (500 μM) in H_2O:DMSO (10:1) at 37 ^oC in the presence of glutathione (5 mM) after (C) 0 h and (D) 24 h incubation.

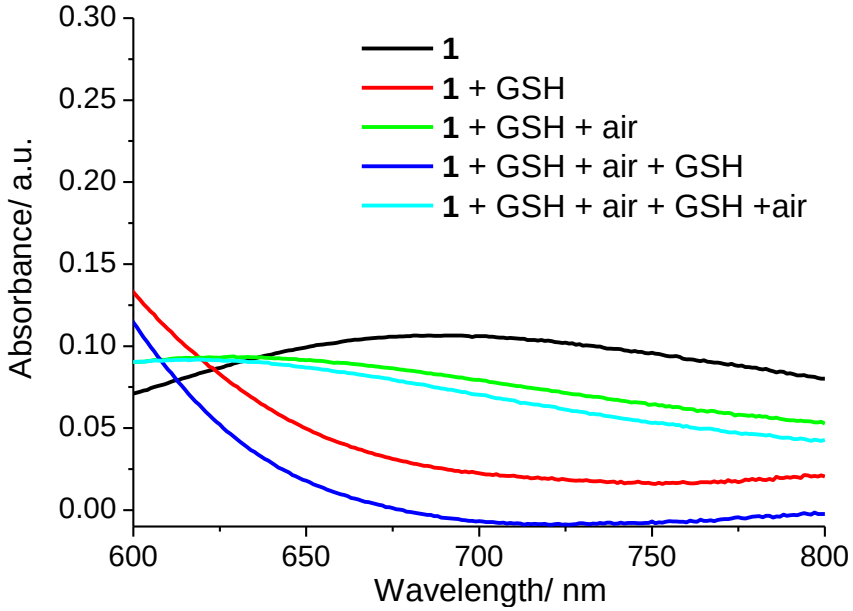

Fig. S18 UV-vis spectra of **1** (1 mM) in DMSO, upon addition of glutathione (1 mM) and exposure to air for 24 h, and further addition of glutathione (1 mM) and exposure to air for 24 h.

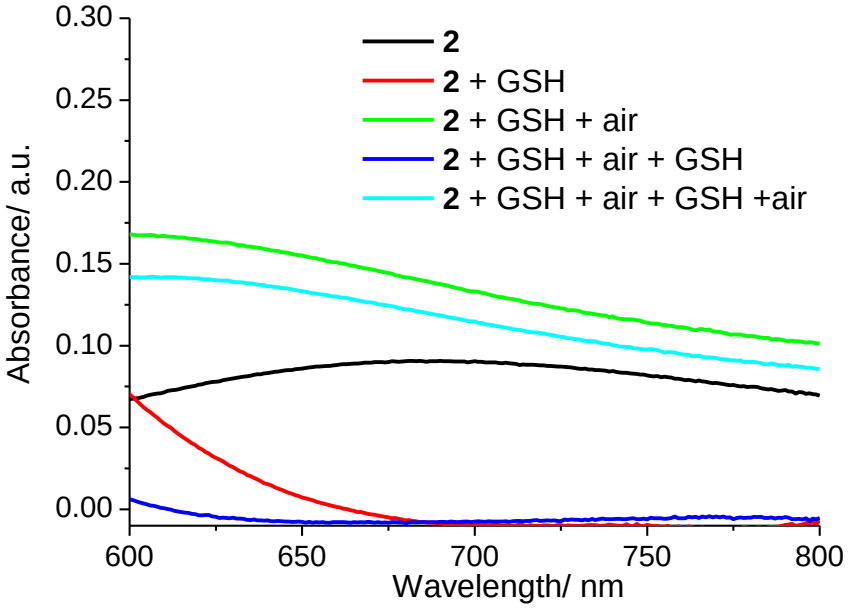

Fig. S19 UV-vis spectra of **2** (1 mM) in DMSO, upon addition of glutathione (1 mM) and exposure to air for 24 h, and further addition of glutathione (1 mM) and exposure to air for 24 h.

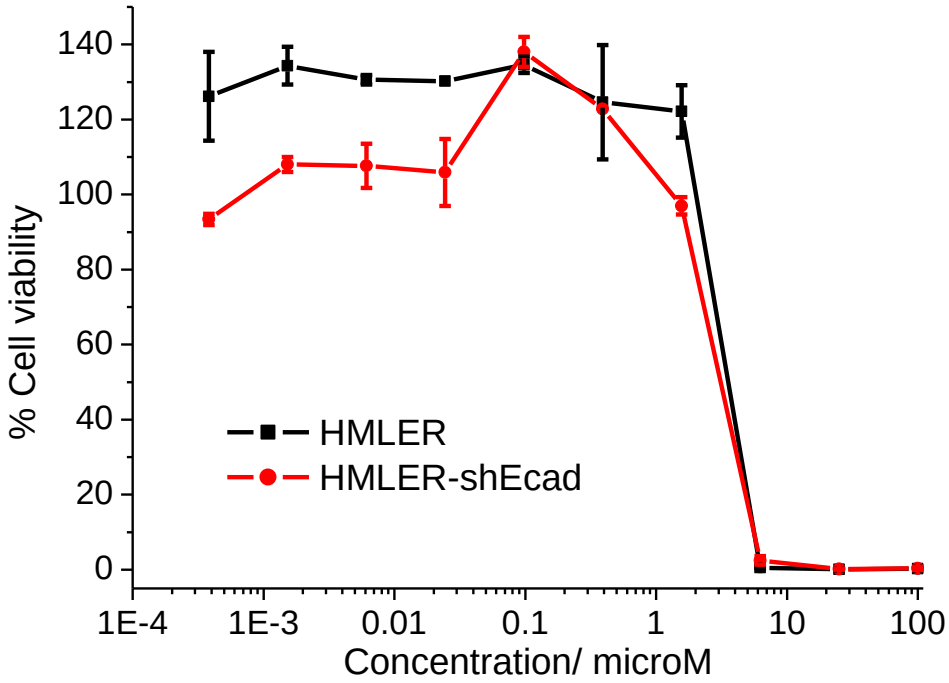

Fig. S20 Representative dose-response curves for the treatment of HMLER and HMLER-shEcad cells with **1** after 72 h incubation.

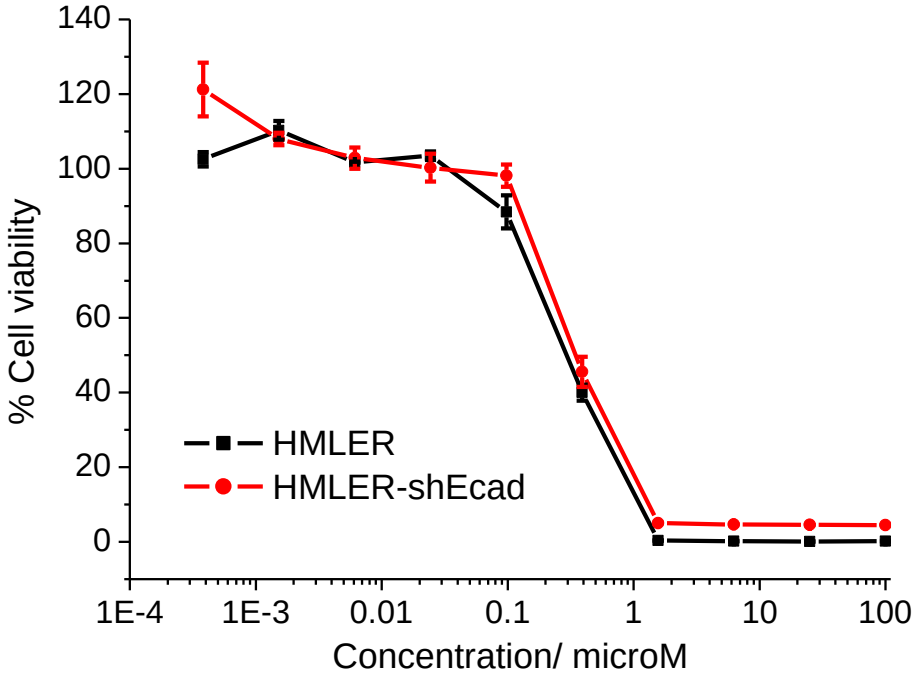

Fig. S21 Representative dose-response curves for the treatment of HMLER and HMLER-shEcad cells with **2** after 72 h incubation.

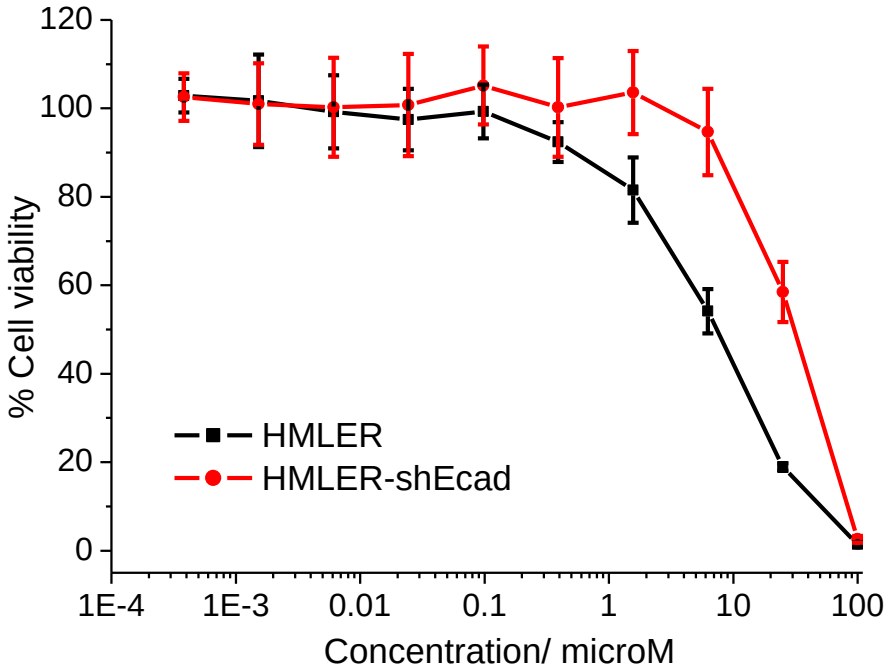

Fig. S22 Representative dose-response curves for the treatment of HMLER and HMLER-shEcad cells with flufenamic acid after 72 h incubation.[7]

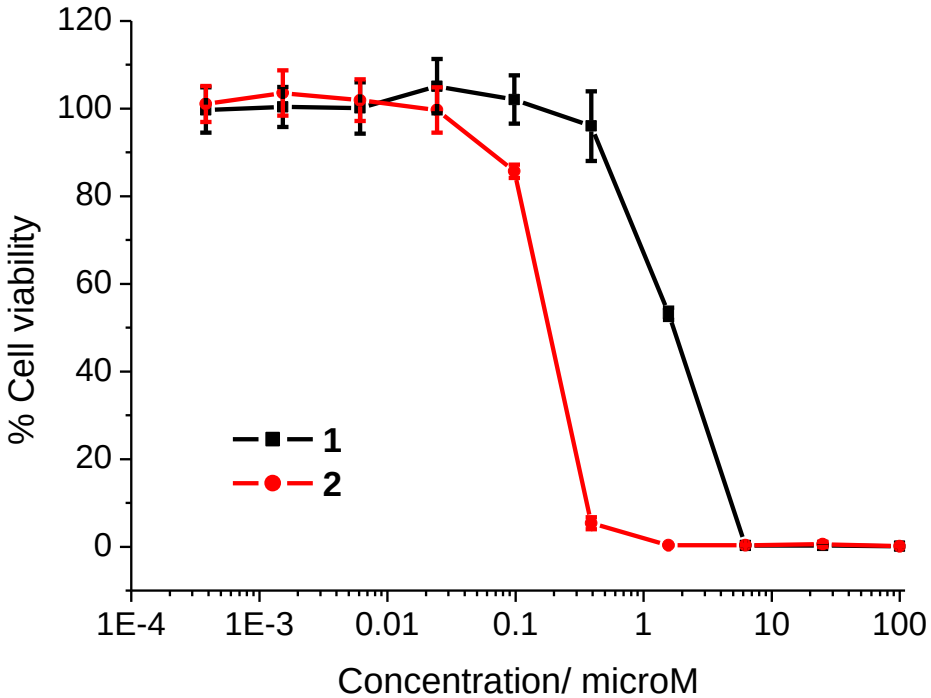

Fig. S23 Representative dose-response curves for the treatment of BEAS-2B cells with **1** and **2** after 72 h incubation.

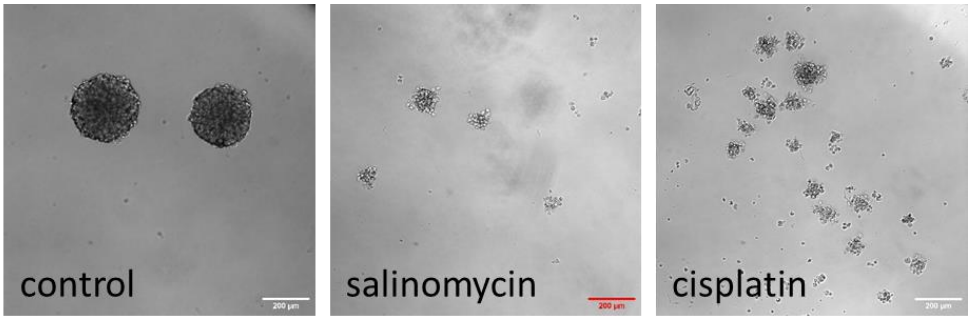

Fig. S24 Representative bright-field images (× 10) of HMLER-shEcad spheroids in the absence and presence of salinomycin or cisplatin at their IC_{20} value (5 days incubation).

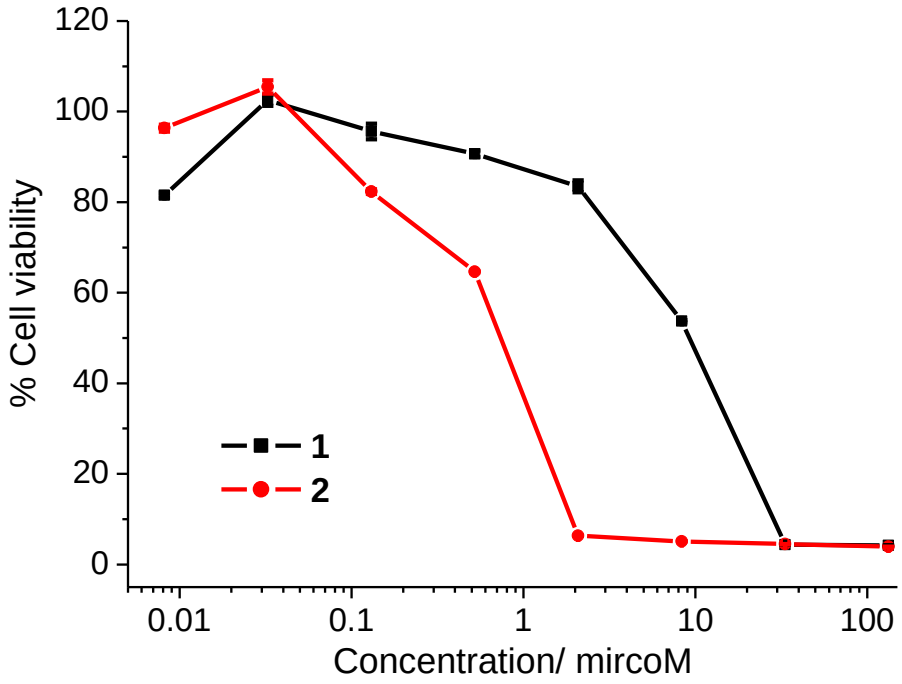

Fig. S25 Representative dose-response curves for the treatment of HMLER-shEcad mammospheres with **1** or **2** after 5 days incubation.

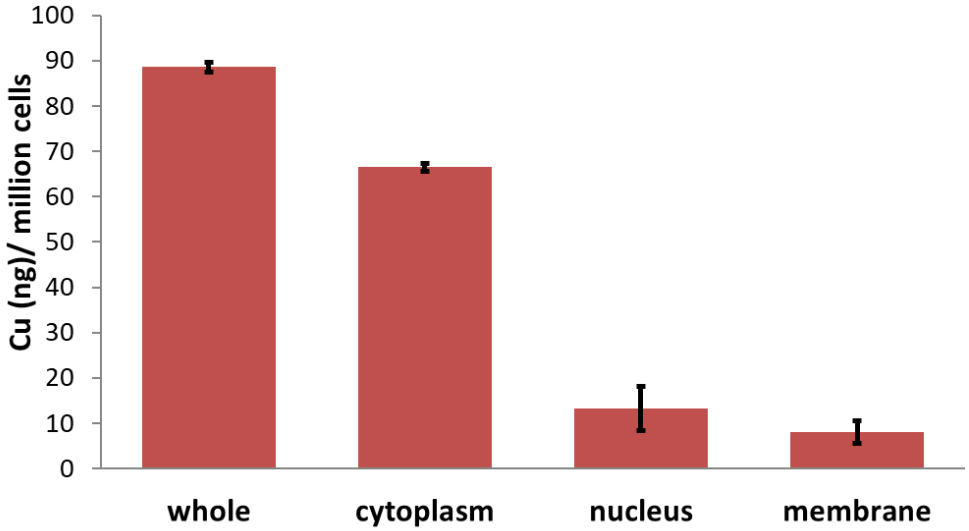

Fig. S26 Copper content (ng of Cu/ 10^6 cells) in various cellular components upon treatment of HMLER-shEcad cells with **2** (1 μM for 24 h).

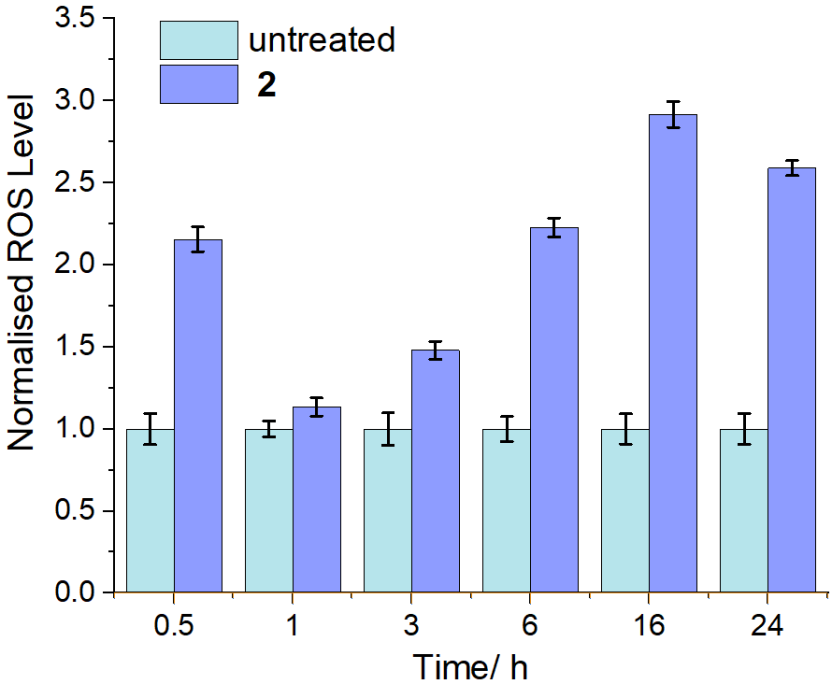

Fig. S27 Normalised ROS activity in untreated HMLER-shEcad cells and HMLER-shEcad cells treated with **2** (2 × IC_{50} value for 0.5, 1, 3, 6, 16, and 24 h).

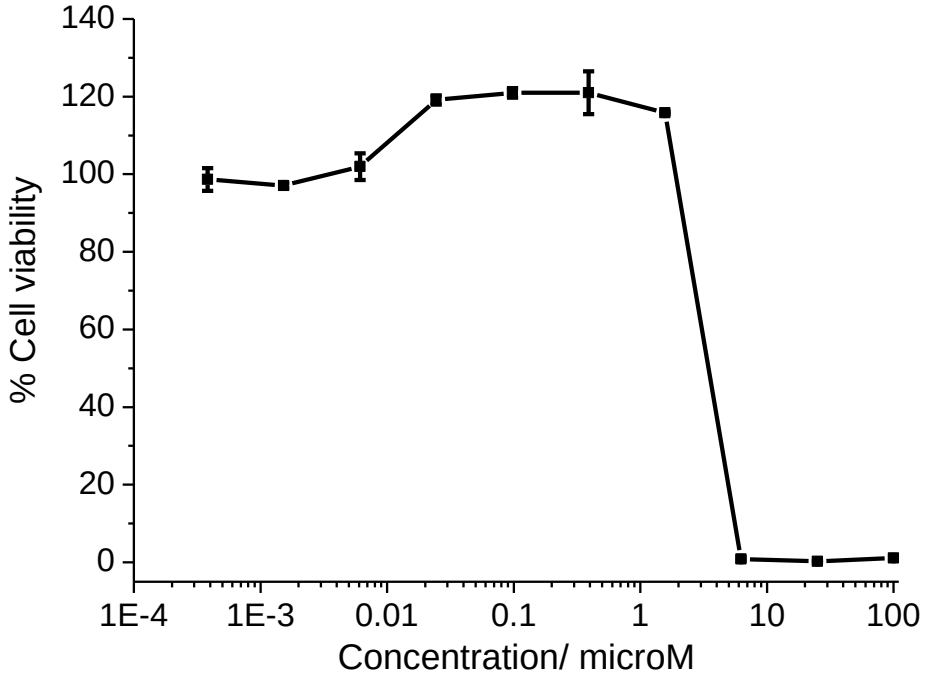

Fig. S28 Representative dose-response curve for the co-treatment of HMLER-shEcad cells with **2** and *N*-acetylcysteine (2 mM) after 72 h incubation.

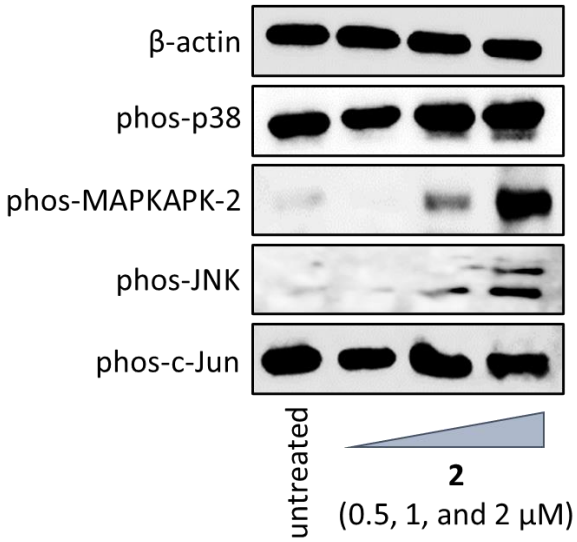

Fig. S29 Immunoblotting analysis of proteins related to the p38 and JNK pathways. Protein expression in HMLER-shEcad cells following treatment with **2** (0.5, 1, and 2 μM for 48 h).

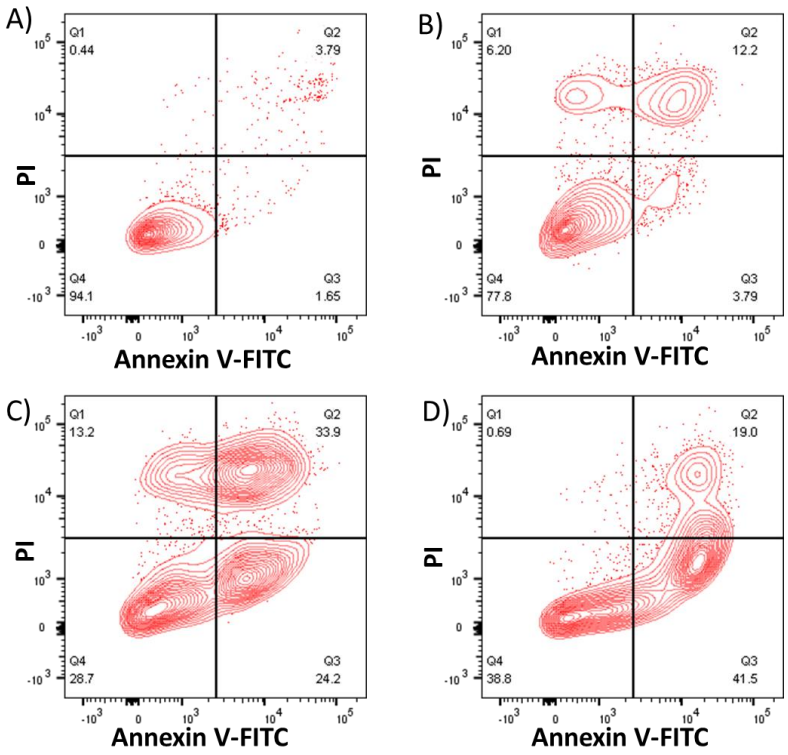

Fig. S30 FITC Annexin V-propidium iodide binding assay plots of (A) untreated HMLER-shEcad cells, (B) HMLER-shEcad cells treated with **2** (2 × IC_{50} value for 72 h), (C) HMLER-shEcad cells treated with **2** (4 × IC_{50} value for 72 h), and (D) HMLER-shEcad cells treated with cisplatin (25 μM for 72 h).

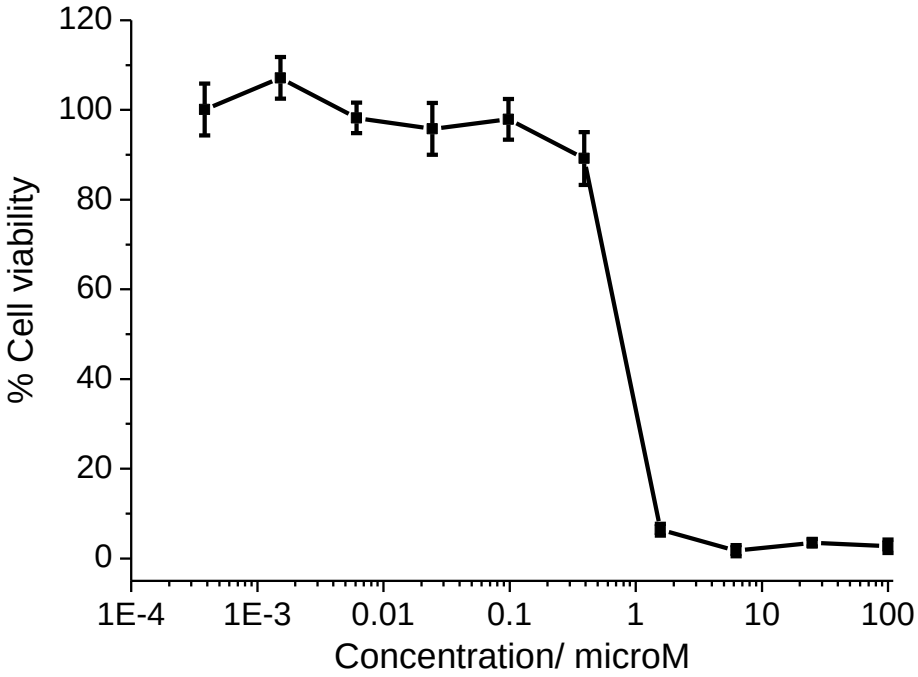

Fig. S31 Representative dose-response curve for the co-treatment of HMLER-shEcad cells with **2** and z-VAD-FMK (5 μM) after 72 h incubation.

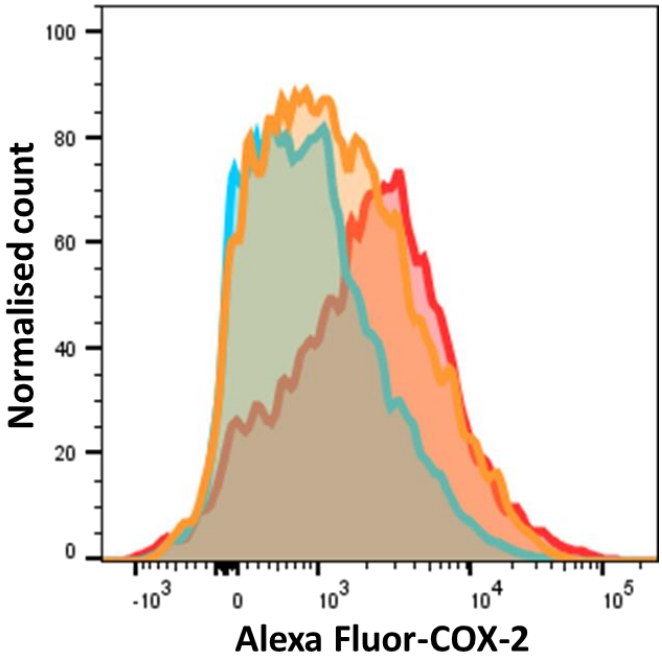

Fig. S32 Representative histograms displaying the green fluorescence emitted by anti-COX-2 Alexa Fluor 488 nm antibody-stained HMLER-shEcad cells treated with LPS (2.5 μM) for 24 h, followed by 48 h in media (red) or media containing **2** (2 × IC_{50} value, blue) or flufenamic acid (20 μM, orange).

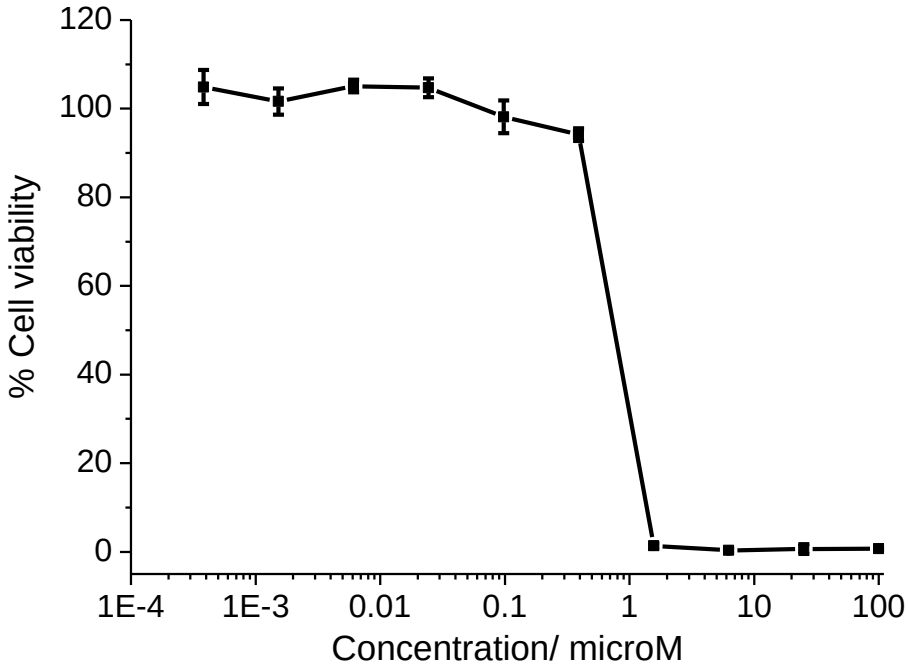

Fig. S33 Representative dose-response curve for the co-treatment of HMLER-shEcad cells with **2** and prostaglandin E2 (20 μM) after 72 h incubation.

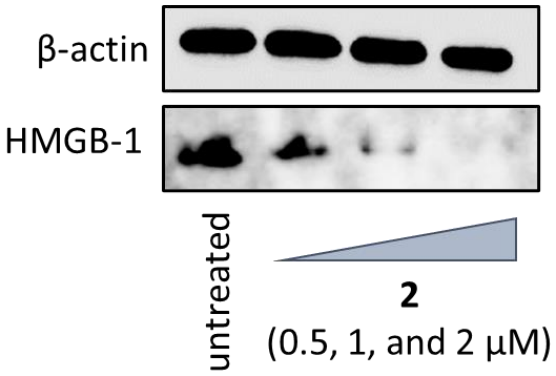

Fig. S34 Immunoblotting analysis of high mobility group box 1 (HMGB-1). Protein expression in HMLER-shEcad cells following treatment with **2** (0.5-2 μM) for 48 h.

References

1. G.M. Sheldrick, *Program for Area Detector Absorption Correction*, Institute for Inorganic Chemistry, University of Göttingen: Göttingen, Germany, 1996.

2. G. M. Sheldrick, *Acta Crystallogr. Sect. A*, 2008, **64**, 112-122.

3. G. M. Sheldrick, *Acta Crystallogr. Sect. C*, 2015, **71**, 3-8.

4. O. V. Dolomanov, L. J. Bourhis, R. J. Gildea, J. A. K. Howard, H. Puschmann, *J. Appl. Crystallogr.*, 2009, **42**, 339-341.

5. L. J. Farrugia, *J. Appl. Crystallogr.*, 2012, **45**, 849-854.

6. *POV-Ray*, Persistence of Vision Raytracer Pty. Ltd.: Williamstown, Australia, 2013.

7. J. Fang, O. Orobator, C. Olelewe, G. Passeri, K. Singh, S. Awuah and K. Suntharalingam, *Angew. Chem. Int. Ed.*, 2023, DOI: 10.1002/anie.202317940.